Synthesis and Characterization of Surface-Initiated Helical Polyisocyanopeptide Brushes

Eunhee Lim,[†] Guoli Tu,[†] Erik Schwartz,[‡] Jeroen J. L. M. Cornelissen,[‡] Alan E. Rowan,[‡] Roeland J. M. Nolte,[‡] and Wilhelm T. S. Huck*,[†]

Melville Laboratory for Polymer Synthesis, Department of Chemistry, University of Cambridge, Lensfield Road, Cambridge CB2 1EW, United Kingdom, Institute for Molecules and Materials, Radboud University, Nijmegen, Toernooiveld 1, 6525 ED, Nijmegen, The Netherlands

Received November 15, 2007; Revised Manuscript Received January 9, 2008

ABSTRACT: This article describes the first surface-initiated polymerization of isocyanide monomers onto various surfaces in a controlled manner. Brushes up to 200 nm could be easily obtained within 3 h of polymerization, and the polymer growth was studied as a function of reaction time, monomer concentration, and growth conditions, using atomic force microscopy (AFM) and ellipsometry. The monomers used in this study contain dipeptide (L,L-Ala−Ala) side groups; circular dichroism (CD) measurements, Fourier transform infrared spectroscopy (FTIR), and AFM confirmed that the well-defined helical conformation was retained in the polyisocyanide brushes with hydrogen bonds along the polymer chains.

Introduction

Polymer brushes have emerged as a powerful tool to control the morphology and properties of polymer thin films. By surface-tethering polymers in sufficiently high grafting densities, the polymer chains are forced to stretch away from the surface, leading to more or less aligned thin polymer films.[1] Such so-called polymer brushes can be used to improve the charge transport properties of films[2] or generate surface coatings that can respond to changes in temperature, pH, salt concentration, and solvent conditions.[3−6] Furthermore, the alignment of the polymer chains allows a rapid and unidirectional response, which is a prerequisite for the development of nanoscale actuators.[7] A further level of control can be achieved when the polymers adopt well-defined conformations. Schouten and co-workers have reported the synthesis of surface grafted poly(L-glutamates) via ring-opening polymerization of *N*-carboxyanhydride (NCA) monomers.[8,9] These polypeptides form helical structures that can be aligned perpendicular to the surface. Such aligned helical polymer brushes have very interesting optical and piezoelectrical properties.[10] In practice, robust alignment is difficult and the NCA polymerization seems to yield rather thin (<25 nm) films. We are therefore interested in exploring routes to grow helical polymer brushes using another major class of helix-forming polymers, i.e., polyisocyanides.

Polyisocyanides have most commonly been prepared by a Ni(II)-catalyzed polymerization, in which the monomers first coordinate to the nickel center and, upon initiation by a nucleophile, link via a series of consecutive insertion reactions.[11] Because of steric crowding, the polymers adopt helical structures and the use of optically active Ni(II) catalysts or enantiopure monomers gives rise to an excess of either left- or right-handed helices.[12] Chiral peptide substituents have been introduced into the polyisocyanide backbone,[13,14] in which the helical backbones are stabilized by hydrogen bonds between amide group forming β-sheet-like arrangements. Moreover, the incorporation of electroactive side groups such as porphyrin, perylene, ferrocene, carbazole, triphenylamine, and tetrathiafulvalene (TTF) offers routes to polymers suitable for optical and electronic applications.[15−17] The helical, chiral, polyisocyanides bearing ferrocenyl groups exhibited reversible conformational changes on electrical stimuli, which would be a promising feature for using these materials in actuators.[18] In this article, we present the first synthesis of polyisocyanide brushes from amine-terminated self-assembled monolayers on various surfaces using a Ni catalyst. By controlling the reaction time, monomer concentration, and growth conditions, brushes up to 250 nm could be prepared. The morphology of the brush films and the helical structure were characterized using atomic force microscopy (AFM), circular dichroism (CD), and Fourier transform infrared spectroscopy (FTIR).

Experimental Section

Materials. 3-Aminopropyltrimethoxysilane (APTS) and 2-aminoethanethiol were purchased from Aldrich and used as obtained. Tetrakis(*tert*-butylisocyanide)nickel(II) perchlorate ((*t*BuNC)$_4$Ni(ClO$_4$)$_2$), L-isocyanoalanyl-L-alanine methyl ester (L,L-IAA) and Ni(II) catalyst **1** (Scheme 1) were synthesized according to literature methods.[19,20]

Synthesis of Ni(II) Catalyst 1. To a suspension of tetrakis(*tert*-butylisocyanide)nickel(II) perchlorate (152 mg, 0.26 mmol) in CH_2Cl_2 (5 mL) was added 60 μL (0.26 mmol, 1 equiv) of 3-(triethoxysilyl)-propan-1-amine. The solution turned red immediately and after a few minutes returned to yellow-orange and the solvent was evaporated, resulting in a sticky yellow-orange powder in quantitative yield. Four conformations for this complex are possible; two are in majority and reported here and one minor conformation was also detected, but not reported.

Mp 37 °C. ^{1}H NMR (δ ppm, $CDCl_3$, 400 MHz): 8.05 (t, 1H, N*H*CH$_2$, $^3J_{HH}$ = 8.0 Hz), 6.90 (m, 1H, N*H*CH$_2$), 7.90, 6.90 (br, 1H, N*H*C(CH$_3$)$_3$), 4.01, 3.37 (m, 2H, NHC*H*$_2$), 3.79, 3.22 (m, 6H, SiOC*H*$_2$CH$_3$), 1.88 (br, 2H, NCH$_2$C*H*$_2$CH$_2$Si), 1.70, 1.65 (s, 9H, NHC(C*H*$_3$)$_3$), 1.53, 1.40 (s, 27, NC(C*H*$_3$)$_3$), 1.18 (m, 9H, SiOCH$_2$C*H*$_3$), 0.69 (m, 2H, NCH$_2$CH$_2$C*H*$_2$Si). ^{13}C NMR (δ ppm, $CDCl_3$, 75 MHz): 178.2, 176.1 (N=C−N), 123.9 (Ni−C=N), 61.0, 60.6 (CNC(CH$_3$)$_3$), 58.6, 58.5 (SiO*C*H$_2$CH$_3$), 56.2, 55.7 (NH*C*(CH$_3$)$_3$), 53.0, 46.6 (NH*C*H$_2$), 31.1, 28.7 (CNHC(*C*H$_3$)$_3$), 29.6, 29.4 (CNC(*C*H$_3$)$_3$), 23.9, 22.0 (NCH$_2$*C*H$_2$CH$_2$Si), 18.4, 18.3

* To whom correspondence should be addressed. E-mail: wtsh2@cam.ac.uk.
[†] University of Cambridge.
[‡] Radboud University.

10.1021/ma702531u CCC: $40.75
Published on Web 02/28/2008

Scheme 1. Synthetic Procedure for Surface-Initiated Polymerization of Polyisocyanopeptide Brushes

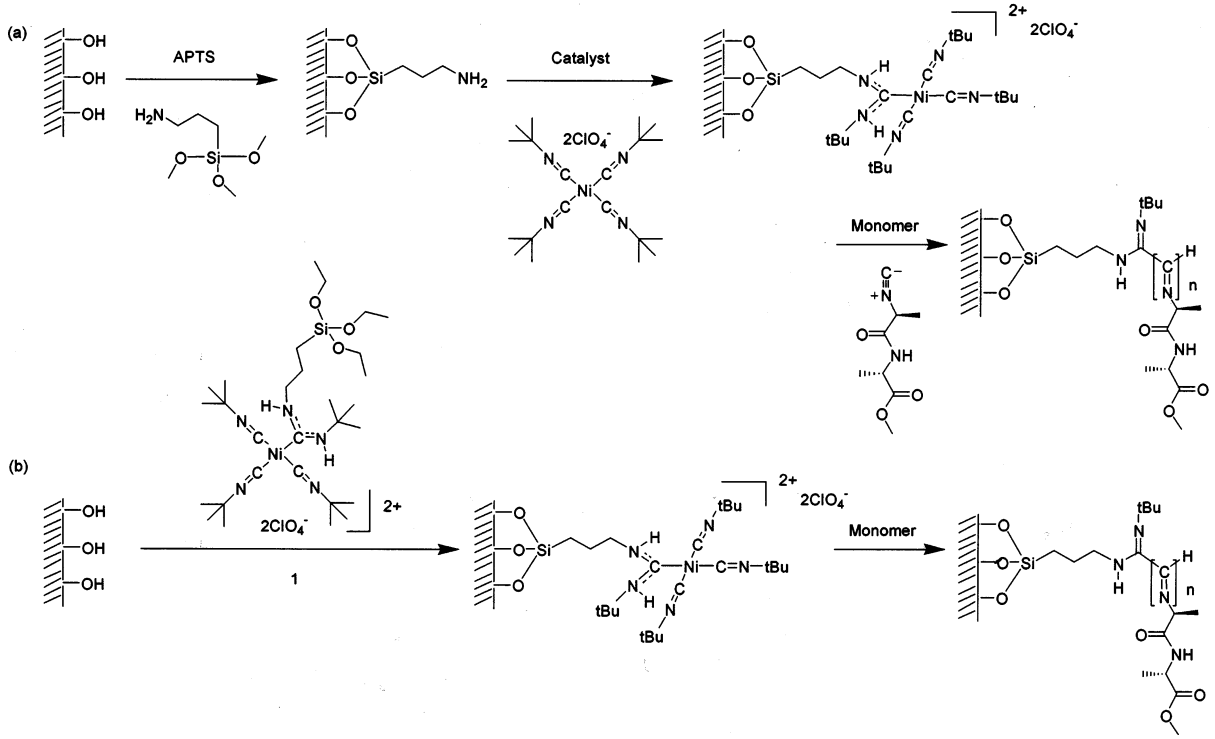

($SiOCH_2CH_3$), 7.4, 7.3 ($NCH_2CH_2CH_2Si$). FT-IR (cm^{-1}, ATR): 3297 (NH), 2975, 2924, 2881 (CH), 2226, 2190 (C═N), 1589, 1546 (NCN), 1191 ($SiOCH_2$), 1073, 622 (ClO_4^-). MS (FAB) *m*/*z*: 710 $(M-ClO_4)^+$.

Formation of Self-Assembled Monolayers (SAMs). Silicon wafers and quartz substrates were cleaned in an O_2 plasma for 20 min and subsequently exposed to APTS vapor, after which the substrates were cured by a baking process. The amino-terminated thiol monolayer was obtained by immersing Au (200 nm, 2 nm Cr adhesion layer) coated Si wafers into a solution of 0.1 M 2-aminoethanethiol in ethyl alcohol for 2 h, after which the substrate was rinsed with ethanol.[21]

Immobilization of Ni(II) Catalyst and Preparation of Polyisocyanide Layer on Substrates. The substrates with amine monolayers were added to a solution of 5 mM $(t\text{BuNC})_4Ni(ClO_4)_2$ (6 mg, 0.01 mmol) in dichloromethane (2 mL) for 15 min (Scheme 1a). Alternatively, the plasma-cleaned silicon wafer was immersed into a solution of 4 mM Ni(II) catalyst (**1**) (6 mg, 0.008 mmol) in dichloromethane (2 mL) (Scheme 1b). The substrates were rinsed thoroughly with chloroform to remove any nonbound catalyst and dried with nitrogen. Subsequently, the polyisocyanide layer was prepared by placing the catalyst-modified substrates in a solution of 48 mM L,L-IAA (14 mg, 0.08 mmol) in dichloromethane (1.5 mL). Finally, the substrate was washed with chloroform and methanol and dried with nitrogen.

Physical Measurements. Film thicknesses and refractive indices (at $\lambda = 632.8$ or 532 nm) were measured using a J.A. Woollam alpha SE ellipsometer using a Cauchy model. Height-mode atomic force microscopy (AFM) images were obtained using a Digital Instruments Nanoscope III, in tapping mode. The root-mean-square (rms) surface roughness of brushes was obtained from AFM images of an area of $3 \times 3\ \mu m^2$. Contact angle measurements were performed using a homemade stage with a computer-controlled microsyringe and a digital camera. Infusion rate of 2 L/min was used, and images for advancing angles were recorded. Circular dichroism (CD) spectra were recorded on an Applied Photophysics Chirascan circular dichroism spectrophotometer at 25 °C. UV−vis absorption spectra were obtained with a Varian 4000 UV−vis spectrophotometer. The PIAA brush film used in these CD and UV−vis measurements was prepared on quartz using dichloromethane as solvent for both initiation and polymerization at the same condition which resulted in the 125 nm thick brush on Si wafer. ^1H NMR and ^{13}C NMR spectra were recorded on an Inova 400 MHz or a Bruker AC-300 MHz instrument (operating 75 MHz), respectively. FT-infrared spectra were recorded on a ThermoMattson IR300 spectrometer equipped with a Harrick ATR unit; PIAA brush film (126 nm) used for IR measurement was prepared on Si wafer using dichloromethane as solvent for both initiation and polymerization. Ni(II) catalyst **1**, monomer IAA, and PIAA bulk polymer were measured as solid. Melting points were measured on a Buchi B-545 and are reported uncorrected. FAB mass spectra were recorded on a VG-7070E mass spectrometer, with 3-nitrobenzyl alcohol as matrix.

Results and Discussion

The synthetic schemes for the surface-initiated polymerization are shown in Scheme 1. We followed two strategies for immobilizing the Ni(II) catalysts to the surface: $(t\text{BuNC})_4Ni(ClO_4)_2$ from solution was allowed to coordinate to amino-terminated SAMs or a triethoxysilane Ni(II) derivative (**1**) was used to form activated Ni-functionalized SAMs directly. The polyisocyanide brushes prepared from the two-step immobilization route (Scheme 1a) resulted in rather thin brushes up to 19 nm. The formation of high-quality APTS SAMs is difficult, and it might well be that the surface density of the Ni(II) catalyst is too low to provide efficient brush growth. Nevertheless, the morphology of these thin polymer films is very interesting, as shown in Figure 1. Very thin (5 nm) brushes (Figure 1a) show a mosslike appearance (rms of 1.2 nm), whereas the 19 nm thick brushes show featherlike bundles (rms of 4.4 nm). This is a most unusual morphology for polymer brush films, which are always featureless except for block copolymer brushes, where rounded features develop upon exposure to different solvents.[22] The very high stiffness (persistence length 76 nm) of the polyisocyanides must be a contributing factor in the development of these structures.[23,24] The thickness of the brush layer is less than the persistence length of the polymer chains, which indicates that the featherlike morphologies observed most likely

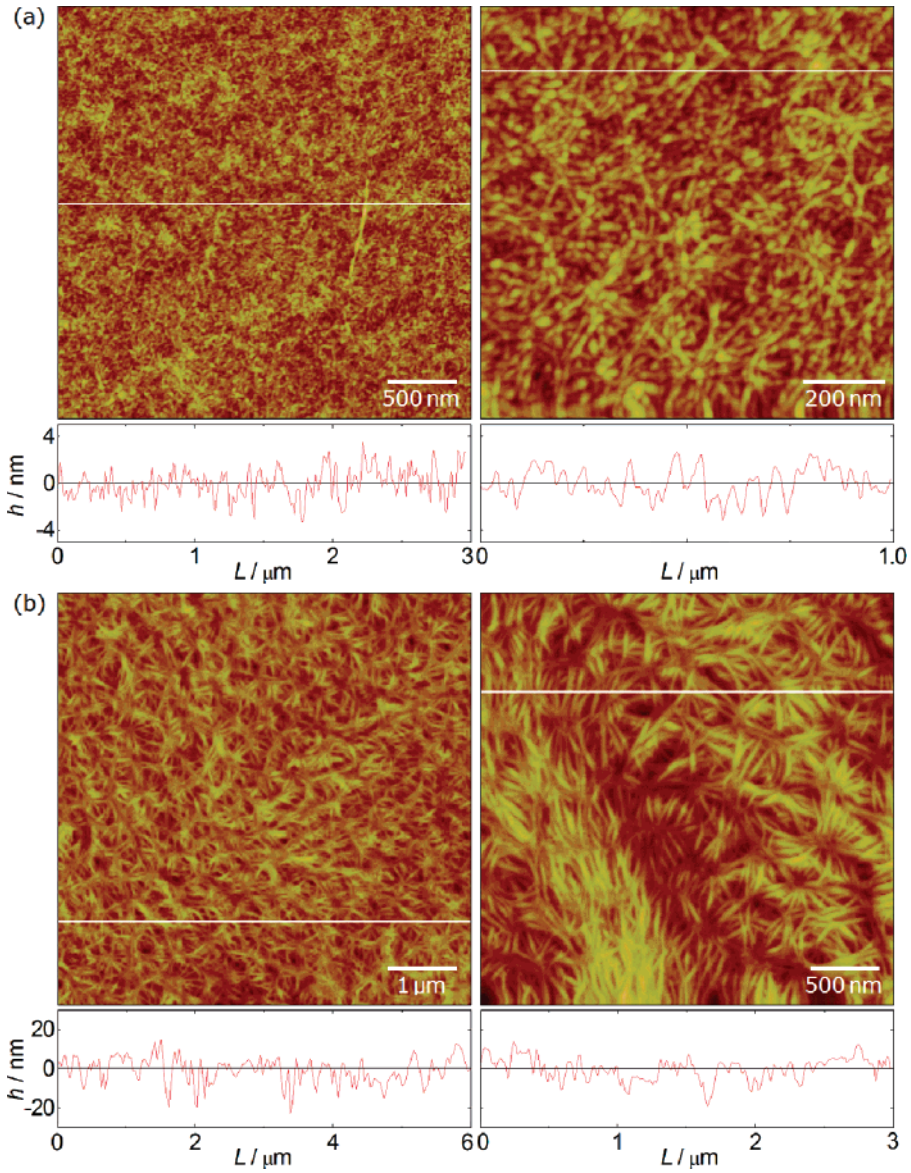

Figure 1. AFM images showing the morphology of PIAA brushes grown on APTS-modified silicon wafers (a) 5 nm thick and (b) 19 nm thick brushes.

Table 1. Film Thickness of PIAA Brushes from Various Reaction Time and Monomer Concentrations[a]

polymerization time [h][b]	thickness [nm][c]		
	16 mM[d]	48 mM[d]	80 mM[d]
0.1	2	8	
0.25	23	30	
0.5	32	47	
1	37	82	147
1.2	45	105	178
2	46	143	
2.5	57	168	
17	162	317	462

[a] Polymerized following the procedure of Scheme 1b. [b] Polymerization time for L,L-IAA after the immobilization of catalyst complex (**1**). [c] Average values for separate brush samples prepared using the same conditions and from at least three spots on each sample. [d] Monomer concentration.

consist of stiff bundles of polyisocyanide chains that are more or less aligned in the *x*,*y*-plane. Careful analysis of the AFM images revealed that the length and width of the feathery patterns are on the order of 220 ± 30 and 32 ± 3 nm (average of over 50 features), respectively.

In addition, exposure of the brushes to toluene resulted in an increase in film thickness from 19 to 34 nm, with a concomitant decrease in refractive index (from 1.52 to 1.30), indicating a much rougher surface. AFM analysis showed indeed an increase in surface roughness and an increase in rms value of 4.4 to over 9. This change in surface morphology is likely related to a different molecular organization before and after solvent treatment.[25]

In order to increase the thickness of the brush layer, the carbene-like Ni(II) complex (**1,** Scheme 1b) was synthesized and immobilized on Si/SiO_2 surfaces. The Ni-functionalized SAMs gave ellispometric thicknesses of about 1.4 nm, which indicates good monolayer formation. These surfaces provided an activated Ni complex and efficient initiation and growth of poly(L-isocyanoalanyl-L-alanine methyl ester) (PIAA) brushes up to 200 nm could be achieved in 3 h. In addition, the refractive index of all brushes as measured by the spectroscopic ellipsometer at wavelengths of 632.8 or 532 nm were found to be 1.52 ± 0.015. Water contact angles for all brushes were found to be around 72°. The polyisocyanide brushes showed no changes in morphologies for samples stored under a N_2 atmosphere for 6 months.

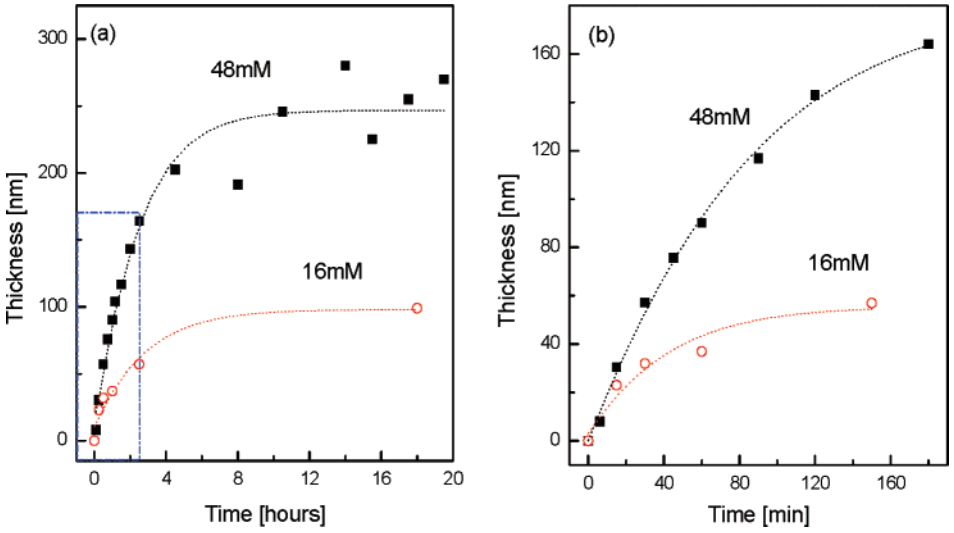

Figure 2. (a) Film thickness as a function of polymerization time using the procedure of Scheme 1b. (b) Zoom-in of part a.

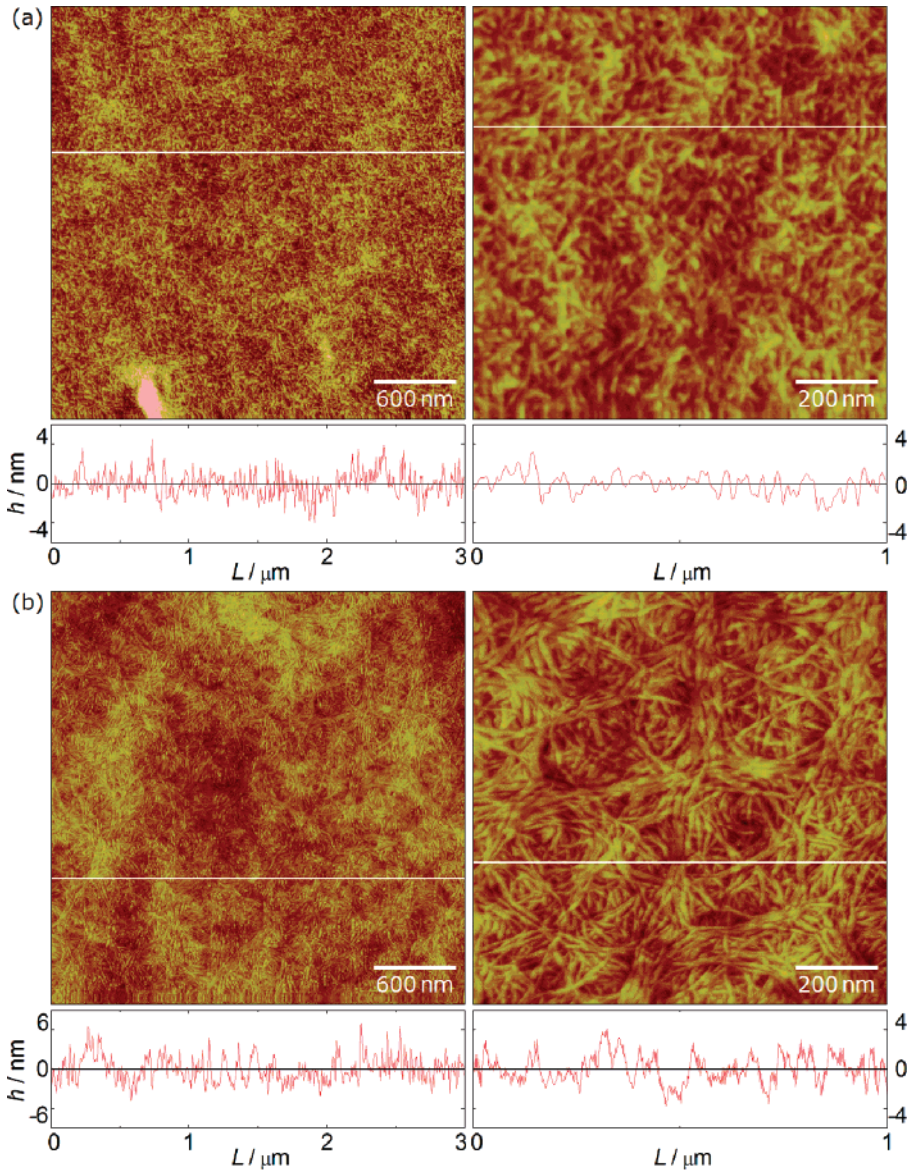

Figure 3. AFM morphology of PIAA brushes grown on a silicon wafer from Ni−SAM with film thicknesses of (a) 56 and (b) 387 nm.

The reaction could be controlled by changing the polymerization reaction time and monomer concentration as shown in Table 1, and no precautions regarding the purification of solvents or the exclusion of oxygen or water were required. Using a monomer concentration of 16 mM, an almost linear dependence of polymer growth vs time was observed (Figure 2) during the

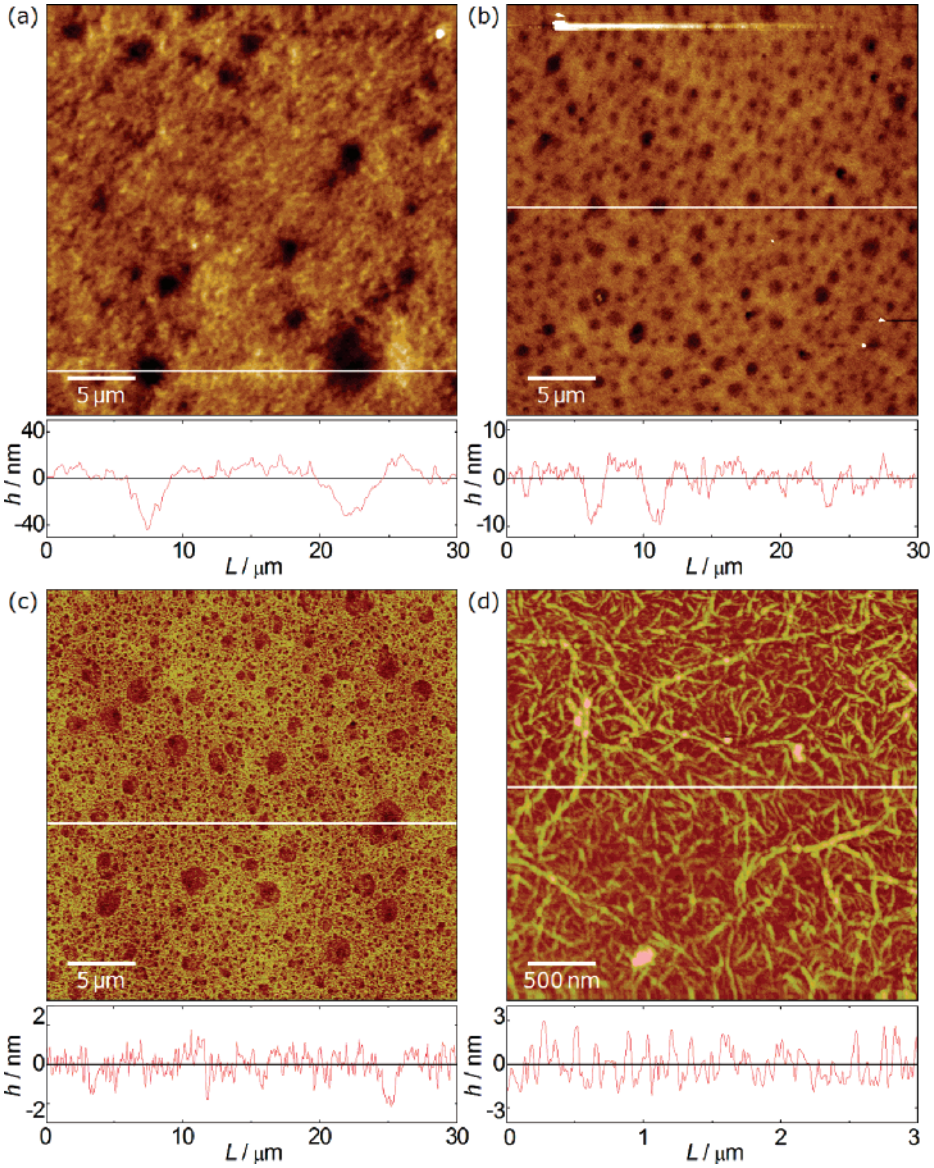

Figure 4. AFM images showing the morphology of PIAA brushes polymerized in (a) EtOAc, (b) toluene, and (c) IPA. (d) AFM morphology of PIAA brushes with low-grafting density.

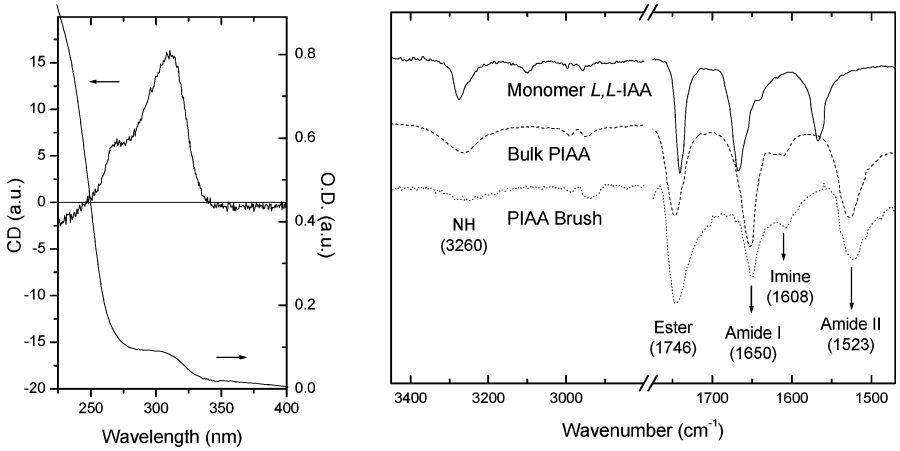

Figure 5. CD/UV−vis spectra of PIAA brushes and FT-IR spectra of monomer L,L-IAA (solid line), PIAA brush (dashed line), and bulk PIAA (dotted line).

first 3 h of the polymerization, leading to ~60 nm thick brushes. After this time, the growth became nonlinear, as is often observed for brush growth using controlled radical polymerizations,[26] indicating competition from termination as well as chain transfer processes. The latter also account for the formation of nongrafted polymeric material, which leads to a slight thickening of the polymerization solution. Thicker brushes could be obtained by using higher (48 mM) monomer concen-

Table 2. Film Thickness of PIAA Brushes Prepared from Various Solvents[a]

solvent		
initiation[b]	polymerization[c]	thickness [nm]
DCM	DCM	161
DCM	EtOAc	220
DCM	toluene	6
DCM	IPA	60
ethyl alcohol	DCM	40
ethyl alcohol	IPA	3

[a] Polymerized following the procedure of Scheme 1b. [b] From a solution containing 4 mM of complex (**1**) for 30 min. [c] From a solution containing 48 mM of L,L-IAA for 3 h.

tration while maintaining the same reaction time (Table 1 and Figure 2).

AFM studies on 56 nm thick brushes (Figure 3a, rms of 1.3 nm) again showed the interesting morphologies already observed on the very thin brushes (Figure 1), whereas the 387 nm thick brushes (Figure 3b, rms of 2.0 nm) exhibited a film morphology without well-defined features. We believe that as these films are much thicker than the persistence length of the chains there is no reason for the chains to align in the plane and the order is lost. Because of the relatively small overall surface areas (1 $\times$ 1 cm^2) and the inherent difficulties with determining molecular weights of stiff polyisocyanides,[27] we did not attempt to elucidate the molecular weights of these polymer brushes, although this would give us valuable information on the grafting density of the films and clues about the orientation of the chains.

The polyisocyanide brush growth is not restricted to silicon wafers but can be realized on gold and quartz substrates as well. To grow brushes on Au-coated silicon wafers, we first formed a 2-aminoethanethiol SAM, followed by immobilization of the Ni catalyst. This procedure yielded very thin films on silicon wafers, but on gold 40 nm thick brushes were obtained after 2 h polymerization time. These brushes showed morphologies similar to the ones grown on silicon wafers and quartz substrates (not shown).

We investigated the influence of different solvents on brush growth and morphology. First, substrates were prepared by forming an initiator SAM via immersion of clean Si wafers in a 4 mM solution of **1** in dichloromethane (DCM). Subsequently, the polymerization was carried out in DCM, ethyl acetate (EtOAc), toluene, or isopropyl alcohol (IPA) for a period of 3 h. The brush thickness results are listed in Table 2, and representative AFM images showing the variation in morphology are shown in Figure 4.

From these results it is clear that toluene and IPA are less ideal solvents for PIAA brush growth, with only 6 and 60 nm thick brushes, respectively, and more importantly, the AFM images show incomplete films with many micron-sized holes penetrating the films. The monomers are only sparingly soluble in these solvents and alcohols (protic solvents) can destroy the nickel initiator complex, which might well explain these results. DCM and EtOAc resulted in robust film growth, but again holes were observed in the case of EtOAc, although these are only $\sim$40 nm deep and do not extend to the substrate.

We then investigated the role of the solvent on the SAM formation and changed DCM for ethyl alcohol (Table 2). Clearly, a significant decrease in brush thickness was observed for both polymerizations in DCM and IPA. The decrease in thickness for the brushes hints at much lower initiator density for EtOH deposited SAMs. The IPA-grown brushes were very thin (3 nm), but the AFM images of these surfaces showed some very interesting structures (see Figure 4d). The ellipsometry data revealed that very little polymer was present, and hence the fibrillar structures seen in Figure 4d must be just a monolayer thick.

A powerful tool to characterize the helical structure of the polyisocyanides is circular dichoism (CD) spectroscopy. When the polypeptides are built from optically pure monomers, an excess of either left- or right-handed helices is expected, and this phenomenon should be visible in the CD spectra in the wavelength range of 250−350 nm, where the n−π* transition of the backbone imine functions reside.[27]

As shown in Figure 5, the CD spectra of our PIAA brushes showed a strong positive single Cotton effect centered at 315 nm, which indicates that the brushes possess right-handed helical structures on the substrate. These helical structures are supported by hydrogen-bonding arrays between the side chains. Strong hydrogen-bonding signals were also present in the IR spectrum, as shown in Figure 5. The peaks at 3260 and 1650 cm^{-1} for the bulk PIAA polymer and the PIAA brush film are attributed to the N−H stretching vibration and amide I vibration, respectively. These peaks have shifted from 3276 and 1667 cm^{-1} for the IAA monomer, implying that the polymer brushes have a structure in which the side chains have an ordered hydrogen-bonding arrangement. A similar investigation was reported in the solid-state IR spectrum of single crystals of the isocyanide monomer, in which the β-sheet-like hydrogen-bonding array between stacked peptide strands was present.[13]

Conclusion

We have reported the controlled surface-initiated growth of helical polyisocyanopeptide brushes using catalytically active monolayers. The synthetic strategy is different from most "grafting from" approaches where the catalyst remains in solution, and only ring-opening metathesis polymerization employs a similar route. The main challenge in these polymerizations is the bond between catalyst and growing polymer chain, and we have shown here how self-assembled monolayer preparation, monomer concentration, and solvents all influence the brush growth. This is the first time that such stiff polymers have been grown from the surface, and we observed very unusual, featherlike morphologies in the brush films. An additional feature of polyisocyanopeptides is the helical nature of the polymer chains. We confirmed that the brushes retain this helical conformation using CD and FT-IR spectroscopy. These polyisocyanide brushes could serve as a new rigid and well-aligned backbone for functional polymer thin films. The unusual, more open, morphologies of these brushes could be exploited by perhaps filling those voids with a second component or could lead to more pronounced surface wetting effects due to increased roughness. We aim to incorporate polyisocyanides with a range of electroactive or biocompatible groups in future work, for the potential development of photovoltaic or piezoelectric materials.

Acknowledgment. This work was supported by the EU Integrated Project NAIMO (No. NMP4-CT-2004-500355). The Council for Chemical Sciences of the Netherlands Organization for Scientific Research (NWO-CW), the Royal Netherlands' Academy for Arts and Sciences (KNAW), and the Technology Foundation STW are acknowledged for financial support. We thank Dr. F. Zhou (University of Cambridge) for his assistance with the preparation of the initiator monolayer.

References and Notes

(1) Edmondson, S.; Osborne, V. L.; Huck, W. T. S. *Chem. Soc. Rev.* **2004**, *33*, 14−23.

(2) Whiting, G. L.; Snaith, H. J.; Khodabakhsh, S.; Andreasen, J. W.; Breiby, D. W.; Nielsen, M. M.; Greenham, N. C.; Friend, R. H.; Huck, W. T. S. *Nano Lett.* **2006**, *6*, 573−578.
(3) Ruhe, J.; Ballauff, M.; Biesalski, M.; Dziezok, P.; Grohn, F.; Johannsmann, D.; Houbenov, N.; Hugenberg, N.; Konradi, R.; Minko, S.; Motornov, M.; Netz, R. R.; Schmidt, M.; Seidel, C.; Stamm, M.; Stephan, T.; Usov, D.; Zhang, H. N. *Adv. Polym. Sci.* **2004**, *165*, 79−150.
(4) Israels, R.; Leermakers, F. A. M.; Fleer, G. J.; Zhulina, E. B. *Macromolecules* **1994**, *27*, 3249−3261.
(5) Raviv, U.; Giasson, S.; Kampf, N.; Gohy, J. F.; Jerome, R.; Klein, J. *Nature (London)* **2003**, *425*, 163−165.
(6) Zhou, F.; Huck, W. T. S. *Phys. Chem. Chem. Phys.* **2006**, *8*, 3815−3823.
(7) Zhou, F.; Shu, W. M.; Welland, M. E.; Huck, W. T. S. *J. Am. Chem. Soc.* **2006**, *128*, 5326−5327.
(8) Wieringa, R. H.; Siesling, E. A.; Geurts, P. F. M.; Werkman, P. J.; Vorenkamp, E. J.; Erb, V.; Stamm, M.; Schouten, A. J. *Langmuir* **2001**, *17*, 6477−6484.
(9) Wieringa, R. H.; Siesling, E. A.; Werkman, P. J.; Angerman, H. J.; Vorenkamp, E. J.; Schouten, A. J. *Langmuir* **2001**, *17*, 6485−8490.
(10) Jaworek, T.; Neher, D.; Wegner, G.; Wieringa, R. H.; Schouten, A. J. *Science* **1998**, *279*, 57−60.
(11) Cornelissen, J. J. L. M.; Rowan, A. E.; Nolte, R. J. M.; Sommerdijk, N. A. J. M. *Chem. Rev.* **2001**, *101*, 4039−4070.
(12) Kajitani, T.; Okoshi, K.; Sakurai, S.-i.; Kumaki, J.; Yashima, E. *J. Am. Chem. Soc.* **2006**, *128*, 708−709.
(13) Cornelissen, J. J. L. M.; Donners, J. J. J. M.; de Gelder, R.; Graswinckel, W. S.; Metselaar, G. A.; Rowan, A. E.; Sommerdijk, N. A. J. M.; Nolte, R. J. M. *Science* **2001**, *293*, 676−680.
(14) Cornelissen, J. J. L. M.; Fischer, M; Sommerdijk, N. A. J. M.; Nolte, R. J. M. *Science* **1998**, *280*, 1427−1430.
(15) Hernando, J.; de Witte, P. A. J.; van Dijk, E. M. H. P.; Korterik, J.; Nolte, R. J. M.; Rowan, A. E.; Garcia-Parajo, M. F.; van Hulst, N. F. *Angew. Chem., Int. Ed.* **2004**, *43*, 4045−4049.
(16) Nishimura, T.; Maeda, K.; Ohsawa, S.; Yashima, E. *Chem.—Eur. J.* **2005**, *11*, 1181.
(17) Gomar-Nadal, E.; Mugica, L.; Vidal-Gancedo, J.; Casado, J.; Navarrete, J. T. L.; Veciana, J.; Rovira, C.; Amabilino, D. B. *Macromolecules* **2007**, *40*, 7521−7531.
(18) Hida. N.; Takei, F.; Onitsuka, K.; Shiga, K.; Asaoka, S.; Iyoda, T.; Takahashi, S. *Angew. Chem., Int. Ed.* **2003**, *42*, 4349−4352.
(19) Stephany, R. W.; Drenth, W. *Pays-Bas* **1972**, *91*, 1453−1458.
(20) Cornelissen, J. J. L. M.; Fischer, M.; van Waes, R.; van Heerbeek, R.; Kamer, P. C. J.; Reek, J. N. H.; Sommerdijk, N. A. J. M.; Nolte, R. J. M. *Polymer* **2004**, *45*, 7417−7430.
(21) Hsia, T. H.; Liao, K. T.; Huang, H. J. *Anal. Chim. Acta* **2005**, *537*, 315−319.
(22) Zhao, B.; Brittain, W. J.; Zhou, W.; Cheng, S. Z. D. *J. Am. Chem. Soc.* **2000**, *122*, 2407−2408.
(23) Samori, P.; Ecker, C.; Gossl, I.; de Witte, P. A. J.; Cornelissen, J. J. L. M.; Metselaar, G. A.; Otten, M. B. J.; Rowan, A. E.; Nolte, R. J. M.; Rabe, J. P. *Macromolecules* **2002**, *35*, 5290−5294.
(24) Zhuang, W.; Ecker, C.; Metselaar, G. A.; Rowan, A. E.; Nolte, R. J. M.; Samori, P.; Rabe, J. P. *Macromolecules* **2005**, *38*, 473−480.
(25) Wang, Y.; Chang, Y. C. *J. Am. Chem. Soc.* **2003**, *125*, 6376−6377.
(26) Jones, D. M.; Huck, W. T. S. *Adv. Mater.* **2001**, *13*, 1256−1259.
(27) Cornelissen, J. J. L. M.; Graswinckel, W. S.; Rowan, A. E.; Sommerdijk, N. A. J. M.; Nolte, R. J. M. *J. Polym. Sci., Part A: Polym. Chem.* **2003**, *41*, 1725−1736.

MA702531U